Patterned Poly(2-hydroxyethyl methacrylate) Brushes on Silicon Surfaces Behave as "Tentacles" To Capture Ferritin from Aqueous Solution

Jem-Kun Chen,*,† Zong-Yan Chen,† Han-Ching Lin,‡ Po-Da Hong,† and Feng-Chih Chang§

Department of Polymer Engineering, National Taiwan University of Science and Technology, 43, Sec 4, Keelung Rd, Taipei 106, Taiwan, National Nano Device Laboratory, No. 26, Prosperity Road I, Science-based Industrial Park, Hsinchu 30078, Taiwan, and Department of Applied Chemistry, National Chiao Tung University, Hsinchu, Taiwan

ABSTRACT We have used a very large scale integration process to generate well-defined patterns of polymerized 2-hydroxyethyl methacrylate (HEMA) on patterned Si(100) surfaces. An atom transfer radical polymerization initiator covalently bonded to the patterned surface was employed for the graft polymerization of HEMA to prepare the poly(2-hydroxyethyl methacrylate) (PHEMA) brushes. After immersing wafers presenting lines of these polymers in water and cyclohexane, we observed brush- and mushroom-like regions, respectively, for the PHEMA brushes, with various pattern resolutions. The PHEMA brushes behaved as "tentacles" that captured ferritin complexes from aqueous solution through entanglement between the brushes and the ferritin proteins, whose ferritins were trapped due to the collapsing of the PHEMA. Using high-resolution scanning electron microscopy, we observed patterned ferritin iron cores on the Si surface after thermal removal of the patterned PHEMA brushes and ferritin protein sheaths.

KEYWORDS: patterned PHEMA brush • VLSI process • ferritin

1. INTRODUCTION

Functionalization of silicon surfaces with organic materials is emerging as an important area in the development of new Si-based devices, such as biomicroelectromechanical systems, three-dimensional micro- and nanomemory chips, and DNA- and protein-based biochips and biosensors (1−3). Stable polymer brushes can provide a substrate with excellent mechanical and chemical protection, alter the electrochemical characteristics of the interface, and provide new pathways for the functionalization of Si surfaces (3−5). One particular advantage that polymer brushes have over spin-coated polymer layers is their superior stability toward solvents and/or harsh conditions (e.g., high temperatures), because they are bonded covalently to the substrates. The use of polymers as building blocks for surface modification allows the preparation of "smart" or responsive surfaces that operate on the basis of conformational changes in the polymer backbones. Micropatterned polymer brushes are finding crucial applications in the development of biochips, microarrays, and microdevices for cell growth, regulation of protein adsorption, and drug delivery (6−8). Several techniques have been developed for fabricating patterned polymer brushes, including microlithography (6, 9) and microcontact printing techniques, developed by Whitesides and co-workers (10). Micropatterning of end-grafted polymer brushes on gold and silica surfaces has been achieved (11). While there have been multiple publications reporting the synthesis and properties of patterned polymer brushes on gold substrates, there have been very few publications on patterned polymer brushes on silica surfaces through e-beam lithography. The applicability of these patterned polymer films has been restricted by their limited stability in solvents, their tendency to undergo subsequent chemical reactions, and difficulties encountered during their preparation over large areas and/or complicated topographies.

Recent advances in biomedicine and biotechnology have led to an increasing demand for materials that can undergo specific biological interactions with their environment. Such behavior requires novel surface functionalization strategies (12). There have been many reports describing the preparation of "graft form"-type polymer brushes through atom transfer radical polymerization (ATRP), by manipulating this technique's living nature and extending its applicability to a variety of monomers (13). Surface-initiated ATRP (SI-ATRP) is an effective method for the production of biomedically and biotechnologically interesting brushes (14−17). Another interesting example is polymer brushes based on N-isopropylacrylamide, which displays a lower critical solution temperature (LCST) behavior and can be switched reversibly from hydrophilic biologically inert states to hydrophobic protein- and cell-adhesive states merely by changing the temperature (18).

Ferritin is a protein complex found in most organisms; it functions principally to sequester excess iron from the cell. Ferritin has a diameter of 12.0 nm; it comprises a 2.0 nm thick protein sheath surrounding a "ferrihydrite" mineral core (19). The protein sheath is composed of 24 individual subunits assembled to give a roughly spherical quaternary structure. The 3-fold sites of contact form hydrophilic channels, through which Fe enters the protein (20). Unlike synthetic polymer coatings on metal (e.g., magnetic) nanoparticles that are biodegradable (21) and, thus, not suitable for implanting, ferritin is naturally occurring, is biocompatible in the body over long periods of time, and does not pose toxicity risks. In this study, we used polymerization to chemically amplify surfaces patterned with a very large scale integration (VLSI) system into patterned poly(2-hydroxyethyl methacrylate) (PHEMA) brushes. We covalently bonded ATRP initiators onto hydroxylated surface patterns, prepared using electron beam lithography and oxygen plasma treatment, and then amplified the system vertically using ATRP. This surface-initiated polymerization process allowed the rapid fabrication of high-resolution patterns of polymers (Figure 1 and Scheme 1). After immersion in water and cyclohexane, we observed distinct brush- and mushroomlike structures, respectively, for the patterned lines of PHEMA brushes. In addition, we used these patterned PHEMA thin films to extract ferritin from fluid systems. After removing the coating proteins from the ferritin complexes and the PHEMA brushes through treatment of the wafers at high temperature, we observed the primary adsorption of patterned iron cores on the Si surface (22).

2. EXPERIMENTAL SECTION

2.1. Materials. Figure 1 and Scheme 1 present our basic strategy for the fabrication of the patterned polymer brushes using the VLSI process. The Si wafer was first treated with hexamethyldisilazane (HMDS) in a thermal evaporator at 90 °C for 30 s to transform the surface hydroxyl (OH) groups into an inert film of $Si(CH_3)_3$ groups. The chemical amplified ArF photoresist, obtained from Sumitomo Chemical Co. (Tokyo, Japan), was then spun onto the HMDS-treated Si wafer at a thickness of 780 nm. E-beam lithography was then used to pattern the photoresist with an array of trenches having dimensions ranging from 500 nm to 10 μm under a dose of 10 μC/cm^2. The sample was then subjected to oxygen plasma treatment (OPT) to form OH groups on the HMDS-treated surface; this process caused the surface to become chemically modified (strongly hydrophilic or polar) only in those areas not covered by the photoresist (23), thereby providing a more wettable surface for the preparation of a self-assembled monolayer (SAM) for graft polymerization, which requires an OH-terminated surface. To immobilize the ATRP initiator ((11-(((2-bromo-2-methyl)propionyl)oxy)undecyl)trichlorosilane, BPOTS), the Si substrate that had been treated with HMDS and oxygen plasma was immersed in a 0.5% (w/v) solution of BPOTS in toluene at 50 °C for 3 h. The BPOTS units assembled selectively onto the bare regions of the Si surface after OPT, where it reacted with SiO and SiOO species. This procedure resulted in a surface patterned with regions of BPOTS for ATRP and regions of photoresist. Single-crystal silicon wafers, Si(100), polished on one side (diameter 6 in.) were supplied by Hitachi, Inc. (Japan) and cut into 2 cm × 2 cm samples. The initiator BPOTS was ordered from HRBio Co. (China). The materials used for graft polymerization—HEMA, copper(I) bromide, and 2,2′-bipyridine
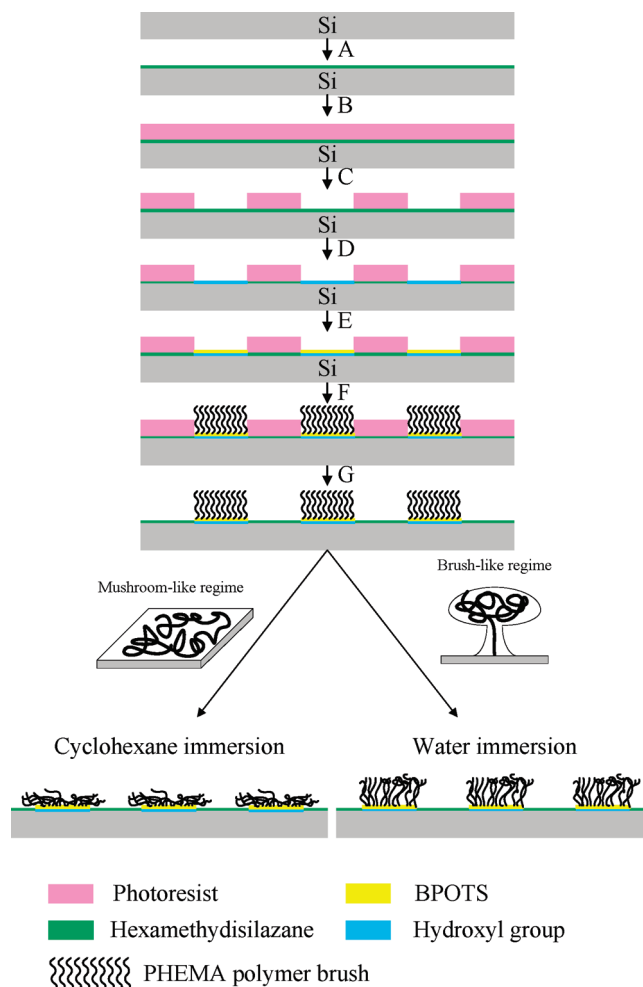

FIGURE 1. Schematic representation of the process used to fabricate surfaces chemically nanopatterned with PHEMA brushes: (A) Si wafer treated with HMDS in a thermal evaporator; (B) photoresist spin-coated onto the Si surface presenting $Si(CH_3)_3$ groups; (C) advanced lithography used to pattern the photoresist with arrays of trenches and contact holes on the surface; (D) oxygen plasma etching used to chemically modify the exposed regions presenting $Si(OCH_3)_3$ groups and to convert the topographic photoresist pattern into a chemical surface pattern; (E) initiator (BPOTS) selectively assembled onto bare regions of the Si surface; (F) sample grafting via surface-initiated ATRP of HEMA from the functionalized areas of the patterned SAM; (G) photoresist removed through treatment with solvent.

(Bip)—were purchased from Acros Organics. HEMA, Bip, and BPOTS were purified through vacuum distillation prior to use. All other chemicals and solvents were of reagent grade and purchased from Aldrich Chemical. All solvents were of reagent grade and were used without further purification. To remove dust particles and organic contaminants, the Si surfaces were ultrasonically rinsed sequentially with methanol, acetone, and dichloromethane for 10 min each and subsequently dried under vacuum. The Si substrates were immersed in hydrofluoric acid (50 wt %) for 5 min at room temperature to remove the silicon oxide film. The HF-treated substrates were then immersed in a mixture of HNO_3 and H_2O_2 (2:1, mol %) for 10 min and subsequently rinsed with doubly distilled water a minimum of five times to oxidize the Si surface. This treatment process reduced the water contact angle of the surface from 45(±1) to 10(±2)°. Polymer-modified Si surfaces were analyzed using ellipsometry (SOPRA SE-5, France) and XPS (Scientific Theta Probe, U.K.).

Scheme 1. Synthetic Route toward PHEMA Brushes Patterned through OPT, Advanced Lithography, and ATRP on Si Wafers
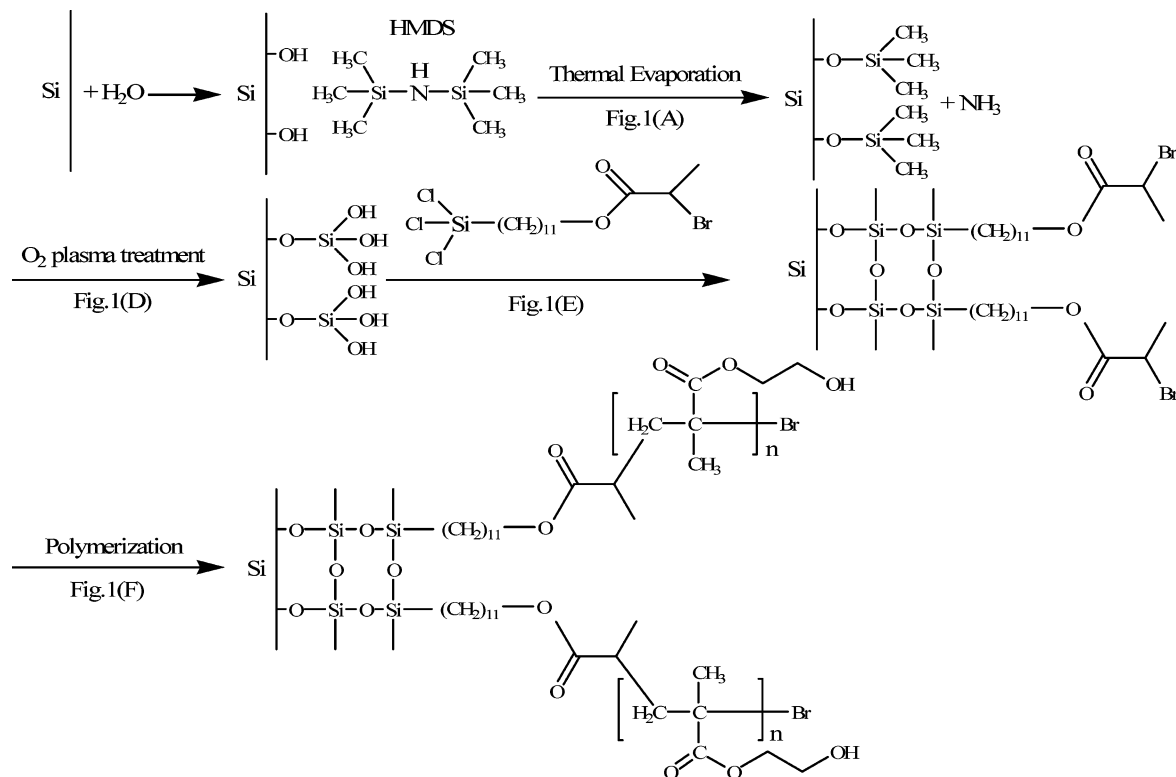
2.2. Initiator-Modified Si Surfaces. Plasma treatment of the Si substrates was performed between two horizontal parallel plate electrodes (area 12 cm × 12 cm). The plasma power supply was 300 W at a frequency of 13.5 MHz. The substrate was placed on the bottom electrode with the Si(100) surface exposed to the glow discharge at an O_2 pressure of ca. 5×10^{-3} Torr for a predetermined period of time to form hydroxyl peroxide species for the subsequent graft polymerization experiment. Because the glow discharge chamber was purged thoroughly with a continuous O_2 stream prior to ignition, residual air or water vapor in the chamber had negligible, if any, effect. The functionalized Si substrates were removed from the solution, washed with toluene for 15 min to remove any unreacted material, dried under a stream of nitrogen, and subjected to surface-initiated polymerization reactions. Finally, the surfaces were dried under vacuum and stored under a dry nitrogen atmosphere.

2.3. Surface-Initiated ATRP. HEMA (10 mL, 82.6 mmol), CuCl (55 mg, 0.55 mmol), $CuBr_2$ (36 mg, 0.16 mmol), and Bip (244 mg, 1.85 mmol) were dissolved in water (10 mL), and then the solution was stirred and degassed with Ar for 20 min. The Si−BPOTS substrate was then added to the solution at room temperature. After various polymerization times, the wafers were placed in a Soxhlet apparatus to remove any unreacted monomer, catalyst, and nongrafted material. The remaining photoresist was removed from the HMDS-treated surface by propylene glycol methyl ether acetate (PGMEA) rinsing, leaving behind the chemically nanopatterned surface, which was dried under vacuum at 80 °C for 20 min. The PHEMA brushes were measured using AFM (Veeco Dimension 5000 Scanning Probe Microscope) and high-resolution scanning electron microscopy (HR-SEM, JEOL JSM-6500F, Japan) with a 25° oblique angle.

2.4. Solvent Treatment and the Adsorption of Ferritin. The resolution of the patterned lines of PHEMA brushes after solvent treatment were measured using AFM and HR-SEM. Ferritin (diameter 13 nm; iron core diameter 7 nm) and ferritin removing agent were obtained from MP Biomedicals. The

sample with ferritins is treated under a moist environment to remove the protein around ferritin by bacteria (*Escherichia coli* cells) digesting. After protein removal of ferritins, the iron cores aggregate without adhesion on the surface. Then the surface was cleaned using cyclohexane to wash away any ferritin that was not absorbed on the PHEMA brushes. Processing at high temperature (500 °C) was performed to remove PHEMA, BPOTS, and the protein sheath of the ferritin units prior to SEM imaging of the absorption of ferritin.

3. RESULTS AND DISCUSSION

3.1. Characterization of Si Surfaces Presenting PHEMA Brushes. The idea behind plasma treatment was to create a very reactive gas environment enclosed under a vacuum. Surfaces in contact with the plasma experience interactions that may result in sputtering and chemical reactions caused by highly reactive radicals, low energy ions, and electrons created in the plasma. Because the chemical properties of Si resemble those of carbon, it can be deduced that OPT of a Si surface, followed by atmospheric exposure, can also introduce some active oxygen species, such as SiO and SiOO units, that increase the O/Si ratio. We used these active oxygen species for reactions with the graft polymerization initiator. The introduction of polar groups through plasma treatment also provided a more wettable surface, as indicated by the decreased contact angle for water from 45(±3) to 5(±3)°.

To prepare polymer brushes, it was necessary for us to immobilize a uniform and dense layer of initiators on the Si surface. We used XPS data (C/Si and O/Si ratios) to determine (Figure 2) the chemical compositions of the Si surfaces at various stages during the surface modification process
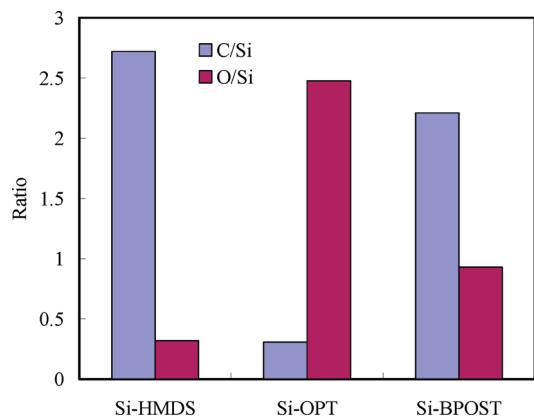
FIGURE 2. O/Si and C/Si atomic ratios of the Si−HMDS, Si−OPT, Si−BPOTS, and Si−PHEMA surfaces, calculated from XPS data.
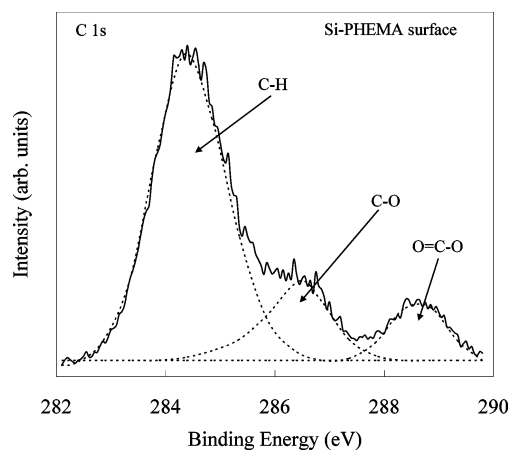

FIGURE 4. Thickness of the PHEMA layer, grown from the Si−BPOTS surface via ATRP, plotted with respect to the polymerization time.

FIGURE 3. XPS C 1s core level spectra of PHEMA brushes grafted from the Si−BPOTS surface for 24 h.

XPS analysis of the Si−BPOTS−PHEMA surface are in fairly good agreement with the respective theoretical ratios.

Ellipsometry and AFM measurements revealed a large increase in film thickness after the growth of the PHEMA layer on the Si−BPOTS surface. We performed control experiments on the Si−H, Si−HMDS, and Si−OPT surfaces using conditions similar to those used for the surface graft polymerization via ATRP. In each case, we observed no discernible increase in the thickness of the control surface. These results confirm that the increase in thickness observed was a result of graft polymerization of the BPOTS-functionalized Si surface. Furthermore, because ATRP is a "living" polymerization process, we expected that the thickness of the polymer brushes would increase linearly upon increasing the polymerization time and the molecular weight of the graft polymer. Figure 4 displays the thicknesses of the PHEMA brushes grafted for various times onto the Si−BPOTS surfaces. We observe approximately linear increases in the thickness of the grafted PHEMA layer on the Si−BPOTS surface upon increasing the polymerization time up to 18 h, providing a so-called brushlike regime of PHEMA brushes. The thickness reached a plateau slightly, indicating the formation of a mushroom-like regime of PHEMA brushes (25). These observations suggest that the PHEMA brushes formed mushroom- and brushlike regimes when the thickness was greater than 364 nm.

3.2. Brush- and Mushroomlike PHEMA Brush Structures on Si Surfaces. In a previous study, we found that polymer brushes transformed into brush- and mushroomlike structures after immersion in good and poor solvents, respectively (25). In our present study, we used water and cyclohexane as the good solvent and poor solvent, respectively, to observe the structural transformation of our PHEMA brushes. For the flat substrate, a PHEMA thin film having a thickness of 424 nm exhibited structure-responsive switching when placed in the good and poor solvents (Figure 5a). After immersion in water, the PHEMA brushes featured predominantly intermolecular hydrogen-bonding interactions with water molecules, providing a hydrophilic PHEMA film. The PHEMA brushes obtained after immersion in

(Si−HMDS, Si−OPT, and Si−BPOTS). Treatment of the pristine Si(100) surface with HMDS passivated the native oxide layer and increased the C/Si ratio, confirming that the Si surface was ideally carbon-terminated after HMDS treatment (24, 25). Additionally, the increasing C/Si ratio and presence in the Br 2p core level spectrum of a signal at a binding energy (BE) of ca. 72.3 eV for the BPOTS-functionalized Si surface indicated that the BPOTS species had been immobilized successfully on the Si surface (25, 26). We used XPS analysis (Figure 3) to investigate the presence of grafted PHEMA brushes on the Si surface. The C 1s core-level spectrum of the PHEMA brushes on the Si surface could be curve-fitted to four peak components having BEs of ca. 284.6, 286.4, and 288.8 eV, attributable to C−H, C−O, and O=C−O species, respectively. The presence of new peaks at ca. 286.4 and 288.8 eV confirmed the presence of the PHEMA brushes on the Si surface. The values of the [N]/[Si] and [C]/[Si] ratios of the Si−HMDS surface obtained from XPS analysis were 0.45 and 2.72, respectively, which are in fairly good agreement with their theoretical ratios of 0.5 and 3, respectively. Fairly good agreements also exist between the XPS-derived and theoretical surface compositions of the Si−OPT and Si−BPOST grafted Si surfaces. For the HEMA homopolymer, the theoretical values of the [O]/[C] and [CH]:[C−O]: [O=C−O] ratios are 0.5 and 4:1:1, respectively. The corresponding ratios of 0.46 and 3.7:1.1:1 that we obtained from
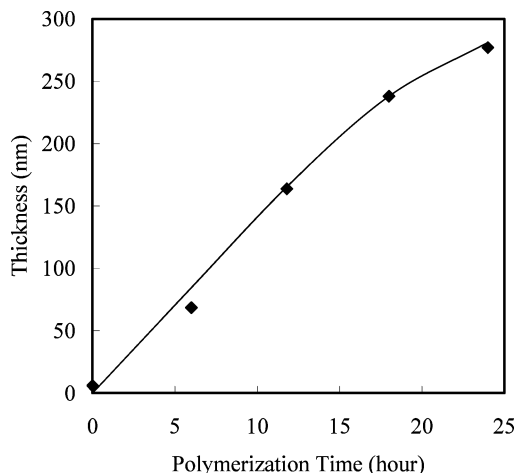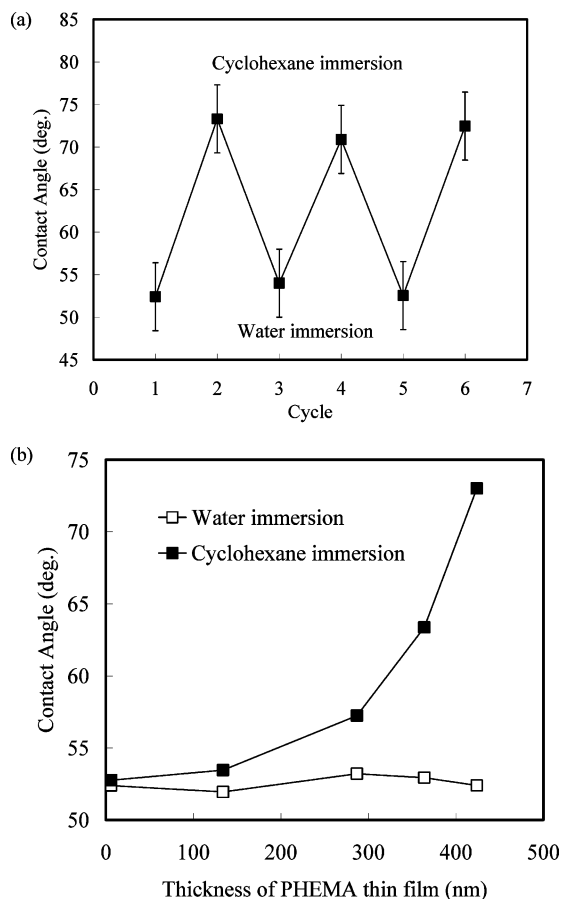
FIGURE 5. (a) Water CAs of brush- and mushroomlike regions of a PHEMA thin film having a thickness of 424 nm after six cycles of immersion in water and cyclohexane. (b) Changes in water CAs after immersion in water and cyclohexane, plotted as a function of the thickness of the PHEMA thin film.

cyclohexane, however, featured intramolecular hydrogen bonding between the C=O and OH groups, resulting in a compact and collapsed conformation of PHEMA chains. The presence of a hydrophilic domain within the PHEMA thin film and the consequent presentation of the alkyl groups of the PHEMA brushes on the surface (27) resulted in the PHEMA film exhibiting slight hydrophobicity after immersion in cyclohexane. Indeed, the water contact angle (CA) of the PHEMA brushes increased from 52(±5) to 73(±5)° after ultrasonic treatment in cyclohexane for 3 h; it returned to 51(±5)° after treating the wafer ultrasonically in water for 3 h. This behavior was reversible for six cycles (Figure 5a) of transformations between the brush- and mushroomlike regimes of PHEMA brushes having a thickness of 424 nm. These results suggest that the solvent-responsive switching between the mushroom- and brush-like regimes was related to the surface chemical composition of this PHEMA thin film. We also investigated the brush- and mushroomlike regimes (in terms of their water CAs) of PHEMA thin films of various thicknesses after immersion in water and cyclohexane (Figure 5b) (28). The water CA underwent clear changes after immersion in water and cyclohexane when the thickness of the PHEMA thin films was greater than 364 nm; i.e., hydrophilic domains formed only within PHEMA thin films possessing appropriately long PHEMA chains,

thereby exhibiting slight hydrophobicity. We suspect that shorter PHEMA chains (film thickness <364 nm) possessed insufficient degrees of freedom to form such hydrophilic domains within their thin films; as a result, they provided similar values for their water CAs after immersion in water and cyclohexane.

We used AFM to visualize the topographies of the PHEMA brushes grafted onto the Si surfaces through ATRP for 24 h and then immersed in the solvents (Figure 6). The root-mean-square surface roughness (R_a) of the pristine Si—H surface was ca. 0.42 nm; the Si—HMDS and Si—OPT surfaces remained molecularly uniform, with values of R_a of ca. 0.48 and 0.53 nm, respectively. After surface treatment with BPOTS, the value of R_a increased slightly to ca. 1.7 nm. These results suggest that ATRP graft polymerization proceeded uniformly on the Si—BPOTS surface to give rise to a dense coverage of PHEMA (29). The PHEMA units on the surface possessed a brushlike structure after immersion in water, as evidenced by an R_a value of ca. 2.1 nm (Figure 6a). The OH groups at the chain ends provided a hydrophilic surface. After immersion in cyclohexane, the PHEMA brushes formed a mushroomlike structure having as R_a value of ca. 0.7 nm (Figure 6b). This decrease in the value of R_a from 2.1 to 0.7 nm confirmed that structural transformations of PHEMA units occurred after immersion of the wafer in these good and poor solvents. The surface presented a mushroom-like structure because of the isotropic or nematic collapse of the PHEMA brushes in the presence of the poor solvent (30). SEM revealed (Figure 6c) the mushroomlike structure of this PHEMA thin film, where the formation of islands having radii of ca. 100 nm presumably resulted from the mushroom-like regime of the PHEMA brushes after they had been grafted for 24 h under vacuum in the SEM chamber.

The final step in our strategy was the surface-initiated polymerization of HEMA from the functionalized areas on the patterned SAM. The presence of reactive OH groups after OPT allowed their direct use in the polymerization step. We used lithography processes with positive photoresists to fabricate trenches having resolutions ranging from 200 nm to 10 μm. We then grafted PHEMA brushes from the Si—BPOTS surfaces of the trenches to form lines of PHEMA brushes. Figure 7 presents the patterned lines of PHEMA brushes grafted for 24 h from trenches having a resolution of 750 nm and then immersed in solvent. Because of the presence of the mushroom- and brushlike regimes, the widths of the lines functionalized with PHEMA brushes had different resolutions after they had been immersed in water and cyclohexane. Using this strategy, the limit of resolution of the patterned PHEMA brushes approached 750 nm. We observed imperfect line patterns for the PHEMA brushes when the trenches had dimensions of less than 750 nm prior to graft polymerization. The AFM images in Figure 7 confirm the success of using the chemical amplification of the patterned OH-functionalized SAM to form spatially localized polymer brushes after immersion in water and cyclohexane. The line pattern of the PHEMA brushes after immersion in water displayed a more irregular overlayer on the surface

ACS APPLIED MATERIALS & INTERFACES
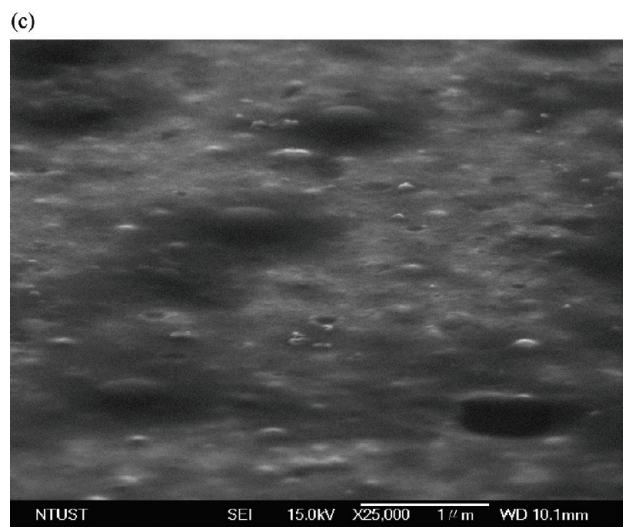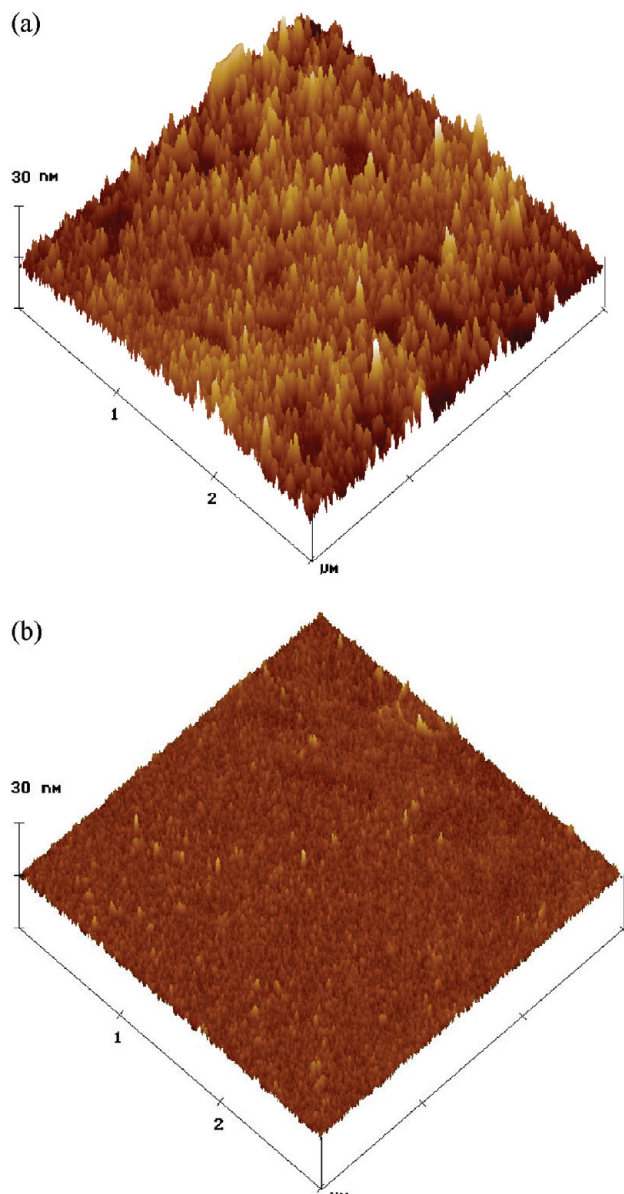
(a)

(b)

(c)

FIGURE 6. (a, b) AFM images of PHEMA brushes obtained after polymerization for 24 h and subsequent immersion in (a) water and (b) cyclohexane. (c) Side-view SEM images (25° oblique angle) of PHEMA brushes having a thickness of 424 nm.
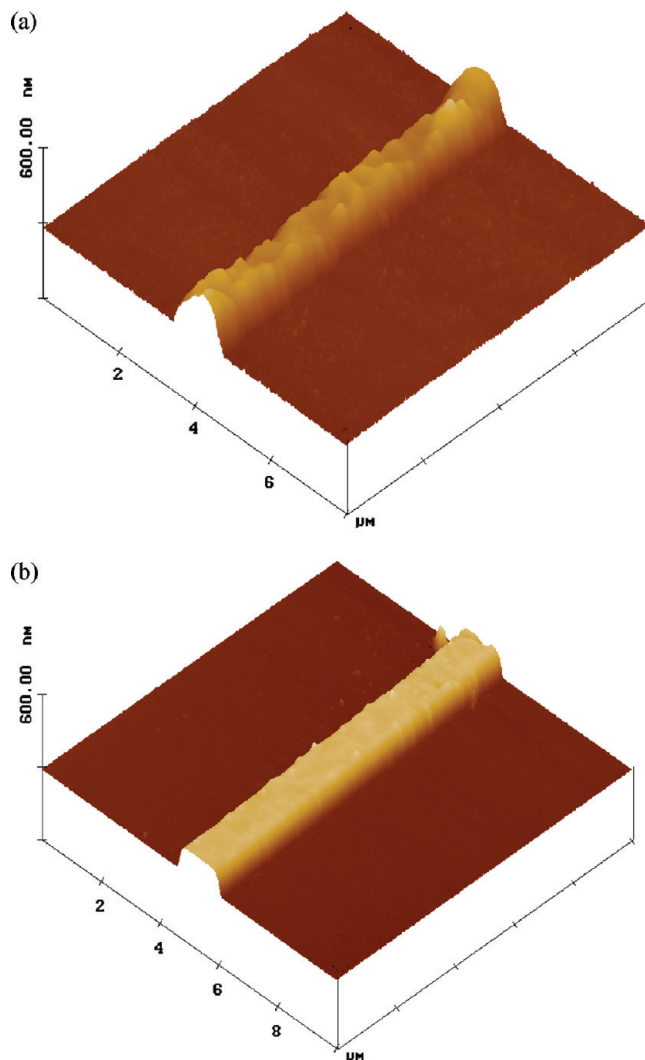
(a)

(b)

FIGURE 7. AFM images of PHEMA brushes grafted from 750 nm trenches for 24 h and then immersed in (a) water and (b) cyclohexane.

because of the brushlike structure of the PHEMA units. After immersion in cyclohexane, a regular line pattern formed because of the interpolymer hydrogen bonding within the mushroomlike PHEMA structures. The line patterns of these PHEMA structures had different heights after treatment in water and cyclohexane because of the presence of the brush- and mushroomlike regimes, respectively. Again, these results confirmed that the thickness of the polymer brushes changed after immersion in the good and poor solvents; furthermore, the grafting density and surface coverage varied accordingly, suggesting that they are both suitable alternative parameters for calculating the thickness. We also used this behavior to establish the "tentacle"-like function of the PHEMA brushes toward ferritin (see below).

3.3. Capturing Ferritin from Aqueous Solution. We exploited the OH groups of the PHEMA brushes obtained after immersion in water as "tentacles" to capture ferritin from aqueous solution (31). Figure 8a displays our strategy for ferritin capture. Using a micropump, we passed an aqueous solution containing dispersed ferritin over the surface presenting the patterned PHEMA brushes, the OH
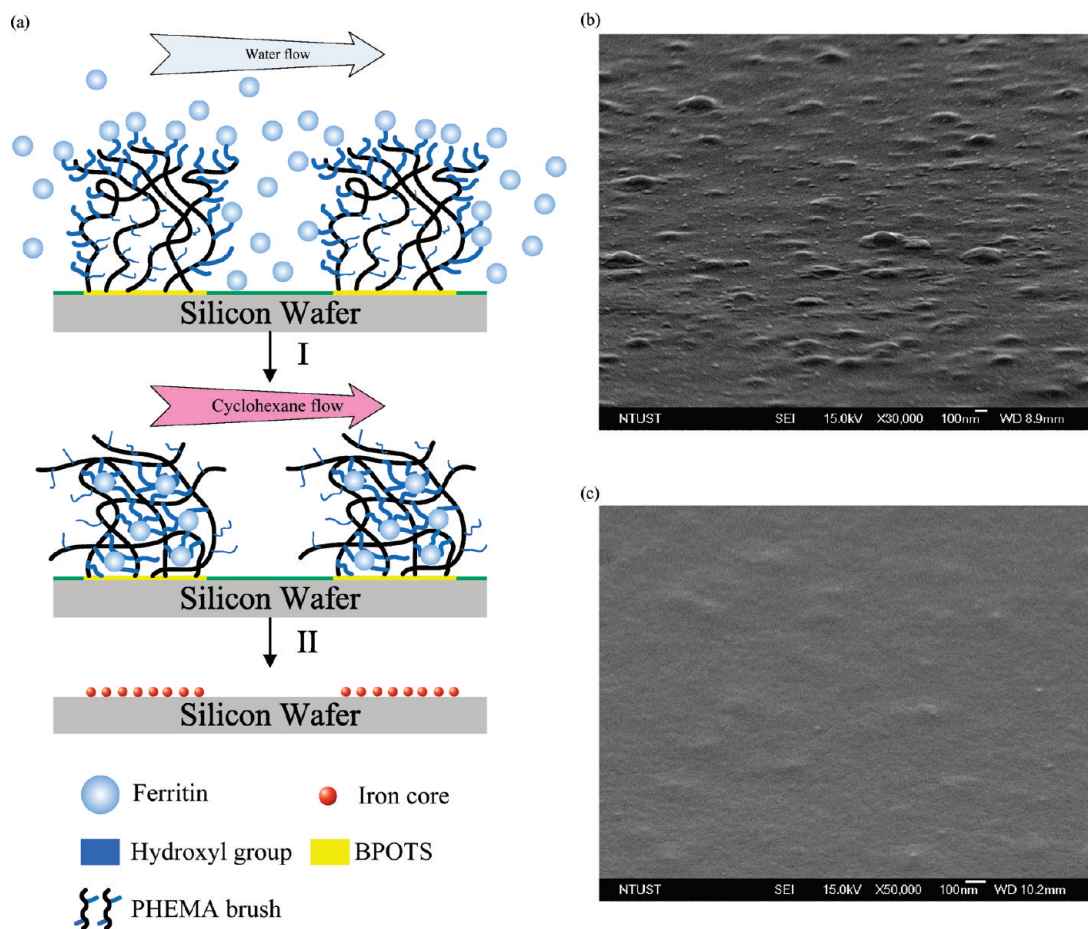
FIGURE 8. (a) Schematic representation of PHEMA brushes behaving as "tentacles" to capture ferritin from aqueous solutions passing over a PHEMA-modified surface: (I) passage of cyclohexane over the PHEMA brushes presenting bound ferritin; (II) removal of nonadsorbed ferritin species and thermal treatment of the wafer at 500 °C for 5 h to remove all organic compounds. (b, c) Side-view SEM images of the PHEMA brushes (thickness 424 nm) obtained after passage of (b) an aqueous solution of ferritin over the wafer surface (45° oblique angle) and (c) cyclohexane over the ferritin-bound surface and subsequent removal of the nonadsorbed ferritin species (25° oblique angle).

groups of which were raised into the solution. It is generally difficult to control protein adsorption on solid surfaces because nonspecific protein adsorption is the first phenomenon when the surface comes in contact with a physiological environment. The "tentacles" captured the ferritin units through entanglement between the OH groups of the PHEMA brushes and the protein sheaths of the ferritin complexes. Next, we passed a cyclohexane solution over the surface to transform it from a brushlike to mushroomlike structure, causing the OH groups of the PHEMA brushes to become buried—along with the associated ferritin units—within the PHEMA thin film to form a hydrophilic domain, whose ferritins were trapped due to the collapsing of the PHEMA. We then removed the ferritin species on the PHEMA thin film surface through degradation of the protein sheath; the buried ferritin units within the thin film were protected by the PHEMA brush under these conditions. The PHEMA brushes and the ferritin protein sheaths buried within them were then removed under oxygen in an oven at ca. 500 °C to observe the ferrihydrite cores.

Figure 8b displays an SEM image of a PHEMA surface prepared through graft polymerization for 24 h and then treated with an aqueous solution of ferritin. The ferritin complexes having radii of 13 nm are clearly visible on the PHEMA surface. After cyclohexane is passed over the PHEMA brush surface and then the surface is cleaned through protein degradation, Figure 8c reveals that only a few ferritin species remained on the PHEMA surface; indeed, most of the ferritin complexes were now buried within the PHEMA thin film. These observations confirmed our notion of PHEMA "tentacles" functioning under the influence of good and poor solvents. In addition, the N 1s core level spectrum recorded after passage of the aqueous ferritin solution over the PHEMA surface displayed a signal at a BE of ca. 400.7 eV, indicating that the ferritin units had been immobilized successfully through interactions with the "tentacles" of the PHEMA brushes on the Si surface. This signal disappeared after passing cyclohexane over the PHEMA surface, consistent with the ferritin complexes having become buried within the PHEMA thin film on the Si surface. To verify this phenomenon, we monitored the distribution of ferritin after treating the PHEMA thin film at 500 °C. The resulting surface displayed two peak components at BEs of ca. 711.8 and 725.7 eV, attributable to Fe—Fe and Fe—O species, respectively, in the Fe 2p core level spectrum (32); in addition, the signal in the N 1s core level spectrum disappeared, confirming that this thermal treatment process decomposed the protein sheaths of the ferritin complexes.
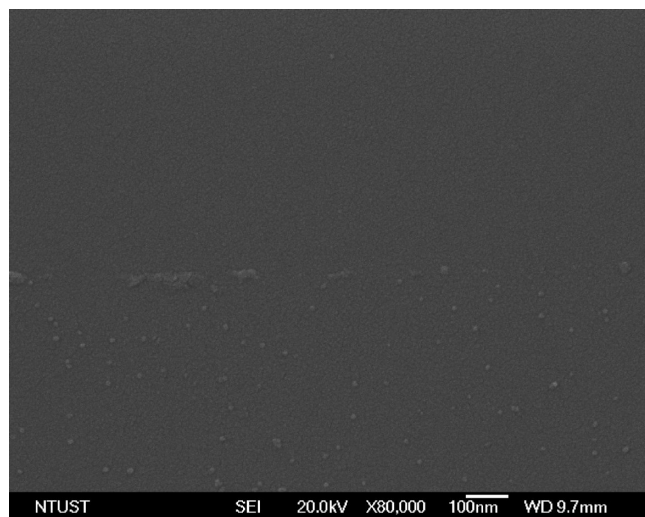
FIGURE 9. Side-view SEM images (45° oblique angle) of the Si surface, the PHEMA brushes grafted through 24 h polymerization from 750 nm wide trenches, and the captured ferritin cores after thermal treatment at 500 °C.

Next, we repeated the procedure using a Si wafer presenting the patterned PHEMA brushes. Figure 9 displays the SEM image we obtained from a patterned PHEMA thin film (grafted from 750 nm wide trenches) after passing an aqueous solution of ferritin over the PHEMA brush surface, passing cyclohexane over the surface, cleaning the surface through protein degradation, and then subjecting the wafer to thermal treatment at 500 °C to remove all organic compounds. The protein sheaths of the ferritin complexes had been removed under these conditions, leaving the iron core units (7 nm radii) on the trenches grafted from the PHEMA brushes. A few remnant PHEMA brushes are visible in Figure 9 around the edges of the 750 nm patterned lines. The regions that had not featured PHEMA brushes presented very few ferritin cores, suggesting that only the PHEMA brushes had captured the ferritin complexes and allowed them to become buried within the thin film when treated with cyclohexane. Our observations reveal that the successful capture and release of biomacromolecules from solution onto Si surfaces is possible when using PHEMA brushes as smart "tentacles" in various solvent systems.

4. CONCLUSION

We have used the "grafting from" system with ATRP to prepare well-defined dense PHEMA brushes on Si wafers through VLSI processing. This novel strategy allows the fabrication of patterned polymer brushes from Si surfaces using commercial semiconductor processes. The key feature of this approach is the use of surface-initiated polymerization through OPT to chemically amplify patterned SAMs into macromolecular films. Because this methodology uses commercial photolithographic tools, it provides patterned polymeric thin films having surface properties that are readily controlled on the nanoscale. In addition, the resolution of the lines formed from the PHEMA brushes can be varied simply by immersion in water or cyclohexane, resulting in brush- and mushroomlike regimes, respectively, of the grafted polymers. We established the ability of the PHEMA

chains to function as "tentacles" for the capture of ferritin complexes from aqueous solution. Our results verify that the protein sheaths of the ferritin units were captured specifically on the PHEMA-patterned areas of the Si surface under aqueous solvents. At present, we are extending this strategy toward the development of protein-detecting devices and are exploring the magnetic properties of iron cores bound to specific areas on Si wafers.

REFERENCES AND NOTES

(1) Lan, S.; Veiseh, M.; Zhang, M. *Biosens. Bioelectron.* **2005**, *20*, 1697.
(2) Buriak, J. M. *Chem. Rev.* **2002**, *102*, 1272.
(3) Létant, S. E.; Hart, B. R.; Kane, S. R.; Hadi, M. Z.; Reynolds, J. G. *Adv. Mater.* **2004**, *16*, 689.
(4) Zhao, B.; Brittain, W. J. *Prog. Polym. Sci.* **2000**, *25*, 677.
(5) Xu, F. J.; Yuan, Z. L.; Kang, E. T.; Neoh, K. G. *Langmuir* **2004**, *20*, 8200.
(6) Andruzzi, L.; Senaratne, W.; Hexemer, A.; Sheets, E. D.; Ilic, S. B.; Kramer, J. K.; Baird, B.; Ober, C. K. *Langmuir* **2005**, *21*, 2495.
(7) Jones, D. M.; Smith, J. R.; Huck, W. T. S.; Alexander, C. *Adv. Mater.* **2002**, *14*, 1130.
(8) Werne, T. A. V.; Germack, D. S.; Hagberg, E. C.; Sheares, V. V.; Hawker, C. J.; Carter, K. R. *J. Am. Chem. Soc.* **2003**, *125*, 3831.
(9) Chen, L.; Zhuang, L.; Deshpande, P.; Chou, S. *Langmuir* **2005**, *21*, 818.
(10) Xia, Y.; Whitesides, G. M. *Angew. Chem., Int. Ed.* **1998**, *37*, 550.
(11) Dyer, D. J. *Adv. Funct. Mater.* **2003**, *13*, 667.
(12) Anderson, D. G.; Burdick, J. A.; Langer, R. *Science* **2004**, *305*, 1923.
(13) Wang, J. Y.; Chen, W.; Liu, A. H.; Lu, G.; Zhang, G.; Zhang, J. H.; Yang, B. *J. Am. Chem. Soc.* **2002**, *124*, 13358–13359.
(14) Mei, Y.; Wu, T.; Xu, C.; Langenbach, K. J.; Elliott, J. T.; Vogt, B. D.; Beers, K. L.; Amis, E. J.; Washburn, N. R. *Langmuir* **2005**, *21*, 12309–12314.
(15) Huang, W.; Baker, G. L.; Bruening, M. L. *Angew. Chem., Int. Ed.* **2001**, *40*, 1510.
(16) Xu, F. J.; Zhong, S. P.; Yung, L. Y. L.; Kang, E. T.; Neoh, K. G. *Biomacromolecules* **2004**, *5*, 2392.
(17) Kizhakkedathu, J. N.; Norris-Jones, R.; Brooks, D. E. *Macromolecules* **2004**, *37*, 734.
(18) Huber, D. L.; Manginell, R. P.; Samara, M. A.; Kim, B.-I.; Bunker, B. C. *Science* **2003**, *301*, 352.
(19) Okuda, M.; Kobayashi, Y.; Suzuki, K.; Sonoda, K.; Kondoh, T.; Wagawa, A.; Yoshimura, H. *Nano Lett.* **2005**, *5*, 991.
(20) Bou-Abdallah, F.; Arosio, P.; Santambrogio, P.; Yang, X.; Janus-Chandler, C.; Chasteen, N. D. *Biochemistry* **2002**, *41*, 11184.
(21) Witte, F.; Feyerabend, F.; Maier, P.; Fischer, J.; Stormer, M.; Blawert, C.; Dietzel, W.; Hort, N. *Biomaterials* **2007**, *28*, 163.
(22) (a) Yoshikawa, C.; Goto, A.; Tsujii, Y.; Fukuda, T.; Kimura, T.; Yamamoto, K.; Kishida, A. *Macromolecules* **2006**, *39*, 2284. (b) Ford, J.; Yang, S. *Chem. Mater.* **2007**, *19*, 5570.
(23) Gehl, B.; Fromsdorf, A.; Aleksandrovic, V.; Schmidt, T.; Pretorius, A.; Flege, J. I.; Bernstorff, S.; Rosenauer, A.; Falta, J.; Weller, H.; Baumer, M. *Adv. Mater.* **2008**, *18*, 2398.
(24) Dong, R.; Krishnan, S.; Baird, B. A.; Lindau, M.; Ober, C. K. *Biomacromolecules* **2007**, *8*, 3082.
(25) Chen, J. K.; Hsieh, C. Y.; Huang, C. F.; Li, P. M.; Kuo, S. W.; Chang, F. C. *Macromolecules* **2008**, *41*, 8729.
(26) Desai, S. M.; Solanky, S. S.; Mandale, A. B.; Rathore, K.; Singh, R. P. *Polymer* **2003**, *44*, 7645.
(27) Xia, F.; Ge, H.; Hou, Y.; Sun, T. L.; Chen, L.; Zhang, G. Z.; Jiang, L. *Adv. Mater.* **2007**, *19*, 2520.
(28) Mei, Y.; Wu, T.; Xu, C.; Langenbach, K. J.; Elliott, J. T.; Vogt, B. D.; Beers, K. L.; Amis, E. J.; Washburn, N. R. *Langmuir* **2005**, *21*, 12309.
(29) Vyas, M. K.; Schneider, K.; Nandan, B.; Stamm, M. *Soft Matter* **2008**, *4*, 1024.
(30) Zhao, B.; Brittain, W. J. *Prog. Polym. Sci.* **2000**, *25*, 677.
(31) Chen, J. K.; Chan, C. H.; Chang, F. C. *Appl. Phys. Lett.* **2008**, *92*, 053108.
(32) Martin, K. C.; Villano, S. M.; McCurdy, P. R.; Zapien, D. C. *Langmuir* **2003**, *19*, 5808.